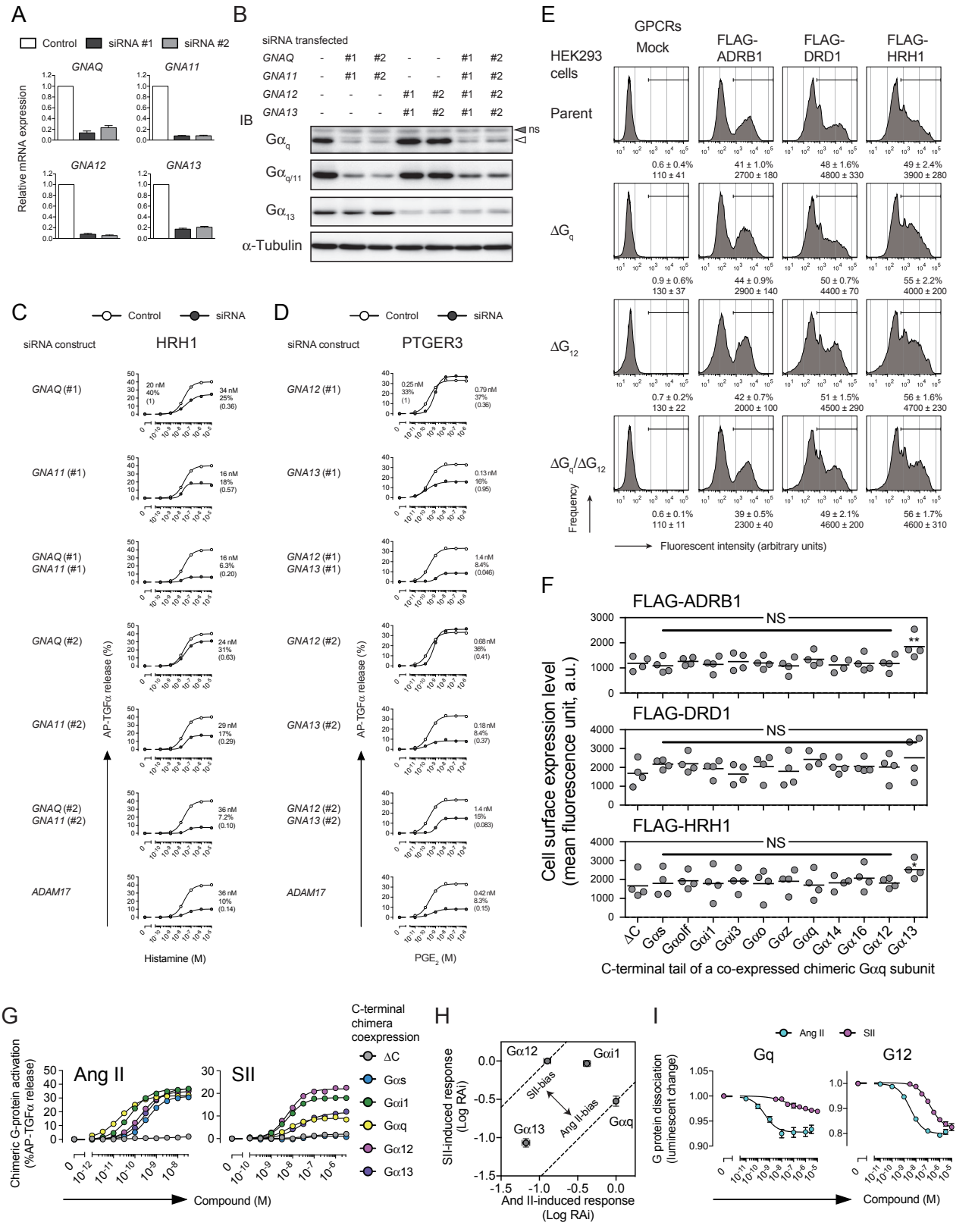

(legend on next page)

Figure S1. Validation of the TGF-α Shedding Assay, Related to Figures 1, 2, and 3

(A) siRNA-mediated knockdown of mRNA expression. HEK293 cells transfected with a siRNA construct specific to each gene (two targeting constructs per gene) were analyzed for mRNA expression by quantitative real-time PCR. The *GNAQ*, the *GNA11*, the *GNA12* and the *GNA13* genes encode $G\alpha_q$, $G\alpha_{11}$, $G\alpha_{12}$, and $G\alpha_{13}$ subunits, respectively. mRNA levels are shown as relative values to that in control siRNA-transected cells. Bars and error bars represent mean and SEM, respectively (n = 3).

(B) siRNA-mediated knockdown at protein expression levels. Lysates from HEK293 cells transfected with a mixture of the indicated siRNA constructs were subjected to immunoblot analyses using antibodies specific to $G\alpha_q$ (an open arrowhead), dually to $G\alpha_q$ and $G\alpha_{11}$ ($G\alpha_{q/11}$), $G\alpha_{13}$ or α-tubulin. Note that owing to a lack of a sensitive, validated antibody against $G\alpha_{12}$, immunoblot for $G\alpha_{12}$ was not assessed. ns, non-specific immunoreactive band (a filled arrowhead).

(C) Knockdown of $G_{q/11}$ attenuates AP-TGF-α release induced by $G_{q/11}$-coupled HRH1. HEK293 cells transfected with a siRNA construct (filled symbols) and an HRH1-encoding plasmid were subjected to the TGF-α shedding assay. Note that the data for the control siRNA (open symbols) are identical in all of the panels. The *ADAM17* gene encode a membrane protease that cleaves the AP-TGF-α reporter protein (Inoue et al., 2012). Numbers to the right of each plot indicate EC_{50}, E_{max} and RAi values obtained from sigmoidal concentration-response curves. Symbols and error bars are mean and SD (three replicate wells per one point), respectively, from a representative experiment of at least two independent experiments with similar results.

(D) Knockdown of $G_{12/13}$ attenuates AP-TGF-α release induced by $G_{12/13}$-coupled PTGER3. Details as for (C), but using another PTGER3 and the corresponding ligand, prostaglandin E_2 (PGE_2).

(E) Parental, ΔG_q, ΔG_{12} and $\Delta G_q/\Delta G_{12}$ HEK293 cells were transiently transfected with a plasmid encoding N-terminally FLAG epitope-tagged GPCR (HRH1, ADRB1 or DRD1) or an empty plasmid (Mock). The transfected cells were stained fluorescently labeled with anti-FLAG tag antibody, followed by a secondary antibody conjugated with a fluorophore, and subjected to flow cytometry analysis. Numbers at bottom of each histogram indicate mean ± SD (four biological replicates) of percentage of receptor-positive cells (a bar region in the histogram) and mean fluorescent intensity (MFI) from a representative of two independent experiments with similar results. Note that due to transient transfection, there are two peaks showing a highly expressing cell pool and poorly expressing one.

(F) In $\Delta G_q/\Delta G_{12}$ HEK293 cells, chimeric Gα subunits were individually transfected with a plasmid encoding an N-terminally FLAG epitope-tagged GPCR (HRH1, ADRB1 or DRD1). The transfected cells were stained fluorescently labeled with anti-FLAG tag antibody, followed by a secondary antibody conjugated with a fluorophore, and subjected to flow cytometry analysis. Plots in the panels denote independent experiments and lines represent mean values (n = 4 or 5). MFI values that significantly differ from the control ($G\alpha_q$ (ΔC)) are denoted by asterisks: *$p < 0.05$, **$p < 0.01$ (one-way ANOVA with Dunnett's post hoc test). NS denotes not significantly different from the control.

(G) Concentration-response curves of AGTR1 for the endogenous ligand (Angiotensin II, AngII) and a biased agonist ([Sar^1-Ile^4-Ile^8] AngII, SII). G-protein signaling activity was assessed by the chimeric-G-protein-based assay. Symbols and error bars are mean and SEM, respectively, of eight independent experiments with each performed triplicate.

(H) Ligand bias plots. For each chimeric-G-protein coupling, LogRAi values were plotted. If SII behaves as a balanced ligand, plots would be linearly aligned. Dotted lines (slope = 1) were drawn crossing C-terminal $G\alpha_q$ or $G\alpha_{12}$ chimera, indicating that SII is more biased toward G_{12} than G_q. Note that activation of $G\alpha_s$ by SII was minimum and thus not included in the plot. Symbols and error bars are mean and SEM, respectively, of eight independent experiments.

(I) Validation of SII bias toward G_{12} by the NanoBiT-G-protein dissociation assay. NanoBiT-G-proteins (G_q and G_{12}) were expressed with AGTR1 and ligand-induced G-protein-dissociation signal was measured. Symbols and error bars are mean and SEM, respectively, of six independent experiments.

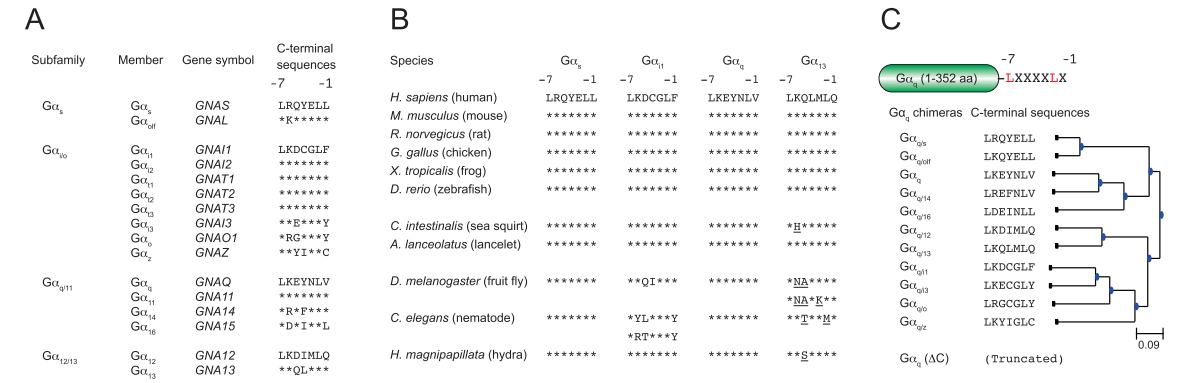

(legend on next page)

Figure S2. Chimeric Gα Subunits and Their Activity for TGF-α Shedding and cAMP Responses, Related to Figures 1, 2, and 3

(A) Seven C-terminal sequences (CGN numbering (Flock et al., 2015) of G.H5.20-G.H5.26) of Gα subunits among the 16 human Gα subunits. Asterisks indicate identical amino acids to one above. Note that there are 11 distinct sequences and that the −7 position (G.H5.20) is a completely conserved leucine.

(B) Evolutionally conservation the seven C-terminal sequences of representative Gα subunits from the four G-protein subfamilies.

(C) Chimeric G-proteins used in this study. We used human $G\alpha_q$-based chimera with a substitution of six C-terminal amino acids. In the negative-control $G\alpha_q$, the seven C-terminal amino acids are truncated.

(D) Capacity of Gα subunits to induce TGF-α shedding response. Scheme of the experiment is shown in left. $G_{i/o}$-coupled DRD2 was co-expressed with an indicated chimeric Gα subunit or a native, full-length Gα subunit in $\Delta G_q/\Delta G_{12}$ cells and subjected to the TGF-α shedding assay by using dopamine. Note that the $G\alpha_{q/i1}$ chimera induced the most potent response and the other negative control conditions ($G\alpha_{i1}$, $G\alpha_q$ or an empty vector transfection (Mock)) did not induce the signal. Symbols and error bars are mean and SD (three wells per one point), respectively, from a representative experiment of at least two independent experiments with similar results.

(E) Capacity of Gα subunits to induce TGF-α shedding response. Scheme of the experiment is shown in left. The experimental design is the same as DRD2, except for usage of G_s-coupled PTGER2, C-terminal $G\alpha_s$ chimeras and prostaglandin E_2 (PGE_2). Note that the $G\alpha_{q/s}$ chimera induced the most potent response and the other negative control conditions ($G\alpha_s$ long isoform ($G\alpha_{sL}$), $G\alpha_s$ short isoform ($G\alpha_{sS}$), $G\alpha_q$ or an empty vector transfection (Mock)) did not induce the signal. Symbols and error bars are mean and SD (three replicate wells per one point), respectively, from a representative experiment of at least two independent experiments with similar results.

(F) Protein expression levels of chimeric $G\alpha_q$ subunits. Lysates from $\Delta G_q/\Delta G_{12}$ cells transfected with a plasmid encoding an indicated chimeric $G\alpha_q$ subunit were subjected to immunoblot analyses using antibodies specific to $G\alpha_q$, $G\alpha_{q/11}$ or α-tubulin. Note that expression levels of the chimeric $G\alpha_q$ subunits were almost equal except for the C-terminally truncated $G\alpha_q$ (ΔC), which was previously shown to undergo spontaneous activation (Denker et al., 1992), and thereby likely to be unstable in cells owing to its tendency to separate from Gβγ subunits.

(G) Kinetics of cAMP level upon G_s-coupled receptor stimulation. HEK293 cells devoid of the G_s subfamily (ΔG_s, lacking $G\alpha_s$ and $G\alpha_{olf}$) (Stallaert et al., 2017) transiently expressing a cAMP biosensor (Glo-22F), a G_s-coupled receptor (AVPR2 or mock transfection) and a $G\alpha_s$ construct (native $G\alpha_s$, $G\alpha_s$-Lg or mock transfection) were loaded with D-luciferin. The cells were stimulated with an increasing concentration of arginine-vasopressin, an AVPR2 ligand, or Forskolin (FSK, 10 μM), an adenylyl cyclase activator, and luminescent signals were measured for 20 min. luminescent signals were normalized to initial counts and relative values are plotted. Each line indicates a kinetics from a single well and data are from a representative experiment of at least three independent experiments with similar results. Note that owing to preference of Forskolin to a $G\alpha_s$-bound adenylyl cyclase (Insel and Ostrom, 2003), Forskolin-induced cAMP response was attenuated in the ΔG_s cells. Also note that in native $G\alpha_s$-expressing cells, owing to higher initial luminescent counts reflecting constitutive G_s activity, amplitude of fold change is smaller than the other conditions.

(H) Concentration-response curves. Fold-change luminescent signals at 10 min after ligand addition in A were normalized to Forskolin response and fitted to a sigmoidal curve. Symbols and error bars are mean and SEM, respectively (n = 3 or 4). Pharmacological parameters are shown at the bottom (mean ± SEM). Mean pEC_{50} values were anti-logarithmically transformed and expressed as pM values in parenthesis.

(I) Chimeric G-protein-based cAMP assay in ΔG_s cells. A test GPCR is expressed together with one of 11 chimeric $G\alpha_s$ subunits harboring C-terminal 6-amino acid substitution in ΔG_s cells and restoration of ligand-induced cAMP response is measured by a luminescent cAMP biosensor. The C-terminally truncated $G\alpha_s$ construct ($G\alpha_s$ (ΔC)) is used for a negative control.

(J) Representative data for the chimeric G-protein-based cAMP assay. TBXA2R was expressed with one of the 11 $G\alpha_s$ constructs or the $G\alpha_s$ (ΔC) and treated with titrated concentration of a ligand (U-46619). Ligand-induced cAMP responses normalized to forskolin (10 μM)-induced response were fitted to a sigmoidal concentration-response curve (upper panels). G-protein coupling is scored as logarithm of RAi values. Symbol size is proportional to E_{max}, which reflects fitting quality. Data for the concentration-response curves are from a representative experiment (mean ± SD of triplicate measurements). Each LogRAi plot denotes single experiment and bars and error bars represent mean and SEM, respectively (n = 5).

(K) Comparison of the chimeric G-protein backbones in coupling profiles. LogRAi values obtained from the chimeric G_q-based TGF-α shedding assay are plotted against the chimeric G_s-based cAMP assay for seven prostanoid receptors. Considered were only mean values for the plots. Note that PTGFR showed poor responses in the cAMP assay and thus not used for the comparison. Linear regression analysis was performed and 90% confidence bands of the best-fit line were shown. Mean ± SD of r^2 values from the seven prostanoid receptors is shown at the bottom.

A

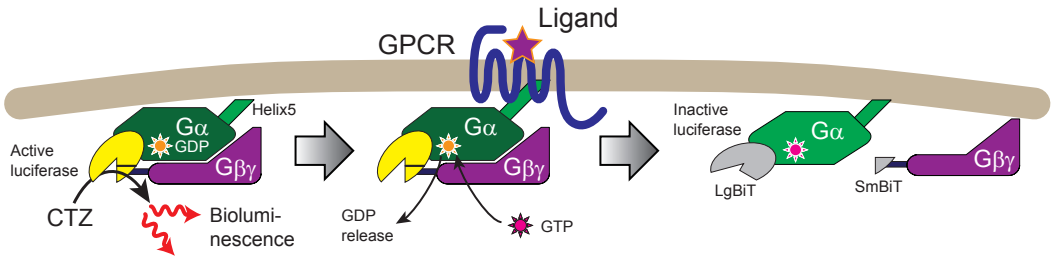

B

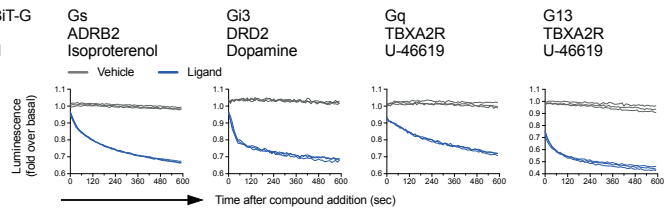

C

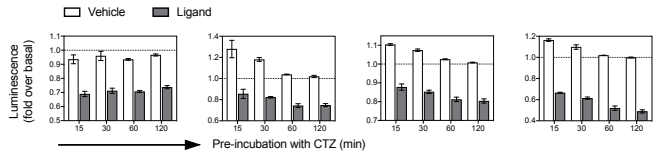

D

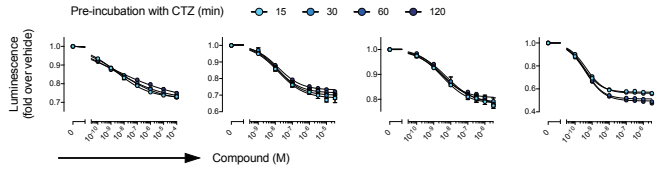

E

Pre-incubation with CTZ (min)	ΔSignal	pEC50	n =	ΔSignal	pEC50	n =	ΔSignal	pEC50	n =	ΔSignal	pEC50	n =
15	0.28 ± 0.01	8.56 ± 0.13 (2.8 nM)	5	0.33 ± 0.03	7.72 ± 0.18 (19 nM)	4	0.22 ± 0.02	8.49 ± 0.09 (3.3 nM)	5	0.43 ± 0.01	9.50 ± 0.02 (0.32 nM)	3
30	0.29 ± 0.01	8.41 ± 0.19 (3.9 nM)	5	0.30 ± 0.01	7.82 ± 0.14 (15 nM)	4	0.21 ± 0.01	8.51 ± 0.03 (3.1 nM)	5	0.44 ± 0.01	9.37 ± 0.06 (0.43 nM)	3
60	0.29 ± 0.01	8.65 ± 0.14 (2.2 nM)	5	0.29 ± 0.02	7.92 ± 0.07 (12 nM)	4	0.19 ± 0.02	8.64 ± 0.03 (2.3 nM)	5	0.49 ± 0.02	9.38 ± 0.03 (0.42 nM)	3
120	0.30 ± 0.01	8.70 ± 0.11 (2.0 nM)	5	0.27 ± 0.01	7.83 ± 0.08 (15 nM)	4	0.20 ± 0.01	8.42 ± 0.05 (3.8 nM)	5	0.50 ± 0.02	9.35 ± 0.05 (0.45 nM)	4

F

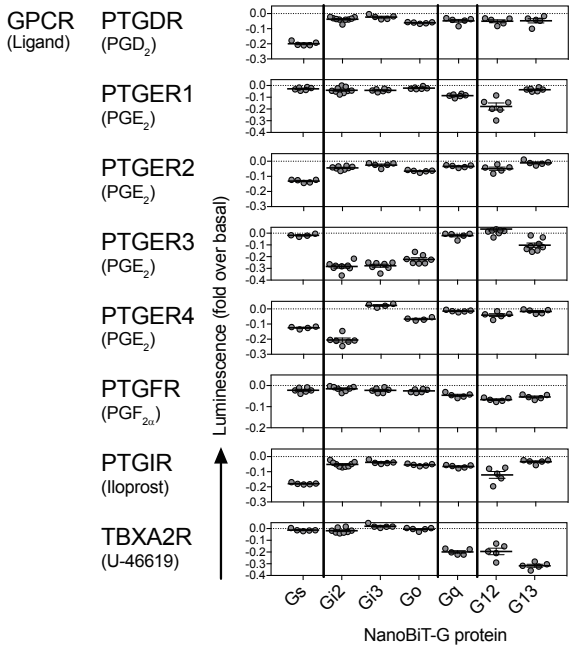

G

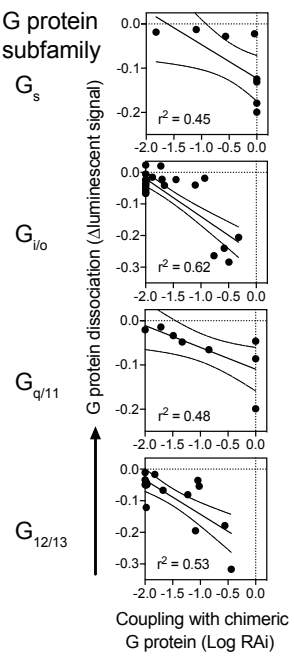

(legend on next page)

Figure S3. Development and Validation of the NanoBiT-G-Protein Dissociation Assay, Related to Figure 1

(A) Scheme of the NanoBiT-G-protein assay. Components of the NanoBiT-G-protein (typically, LgBiT-inserted Gα subunit, SmBiT-fused $G\beta_1$ subunit and native $G\gamma_2$ subunit) and a test GPCR are transiently expressed in HEK293 cells. By loading with coelenterazine (CTZ), a substrate for the NanoBiT luciferase, the NanoBiT-G-protein emits bioluminescence. Stimulation with a GPCR ligand triggers exchange of a guanine nucleotide (GDP release and GTP incorporation) of the NanoBiT-G-protein and induces dissociation of Gα-Lg from Sm-Gβγ, thereby reducing bioluminescence signals. Note that both Gα and Gβγ subunits are lipidated (not shown) and localized to membrane.

(B) Luminescent kinetics of NanoBiT-G-proteins after GPCR ligand stimulation. Representative members (G_s, G_{i3}, G_q and G_{13}) from the four G-protein subfamilies were co-expressed with a corresponding coupling GPCR and stimulated with its ligand (10 μM isoproterenol, 10 μM dopamine or 1 μM U-46119) or vehicle. After ligand addition, a microplate was measured at 10 s interval for 10 min. Each line indicates a luminescent trace of one well, normalized to an initial count, from a representative experiment of at least three independent experiments with similar results. Note that due to a time lag between manual ligand addition and beginning of measurement, NanoBiT-G_{13} shows already dissociated signal from the initial reading.

(C-E) Effect of preincubation time with CTZ. Cells expressing the indicated combination of the NanoBiT-G-protein and the test GPCR were loaded with CTZ for 15-120 min before measurements (baseline and ligand stimulation). Luminescent signals after 3-5 min ligand addition (10 μM isoproterenol, 10 μM dopamine or 1 μM U-46119) or vehicle treatment were normalized to the baseline signals (C). Bars and error bars represent mean and SEM of indicated numbers of independent experiments in E. Changes in the luminescent signals across titrated ligand concentrations were further normalized to that of vehicle treatment and expressed as concentration-response curves (D). Symbols and error bars represent mean and SEM of indicated numbers of independent experiments in E. Parameters (signal changes and pEC_{50} values) were calculated from the sigmoidal curves (E). Data are expressed as mean ± SEM of indicated numbers of independent experiments. Mean pEC_{50} values were anti-logarithmically transformed and expressed as nM values.

(F) Validation of the NanoBiT-G-proteins by using prostanoid receptors. Seven NanoBiT-G-protein (G_s, G_{i2}, G_{i3}, G_o, G_q, G_{12} and G_{13}) were profiled for the eight prostanoid receptors with their ligands shown in parentheses. Each dot represent data from independent experiments and lines and error bars indicate mean and SEM (n = 5-9).

(G) Comparison of coupling profiling between the chimeric G-protein-based TGF-α shedding assay and NanoBiT-G-protein assay. LogRAi values obtained from the chimeric G-protein-based assay are plotted against G-protein dissociation signals from the NanoBiT-G-protein assay for the eight prostanoid receptors. Considered were only mean values for the plots. The G_i family contains data for three members ($G\alpha_{q/i1}$, $G\alpha_{q/i3}$ and $G\alpha_{q/o}$ chimeras; NanoBiT-G_{i2}, NanoBiT-G_{i3} and NanoBiT-G_o, respectively) and the G_{12} family includes data for two members ($G\alpha_{q/12}$ and $G\alpha_{q/13}$ chimeras; NanoBiT-G_{12} and NanoBiT-G_{13}, respectively). PTGER3-G_{12} data were excluded owing to the increased luminescent signal. Linear regression analysis was performed and 95% confident bands of the best-fit lines intervals were shown.

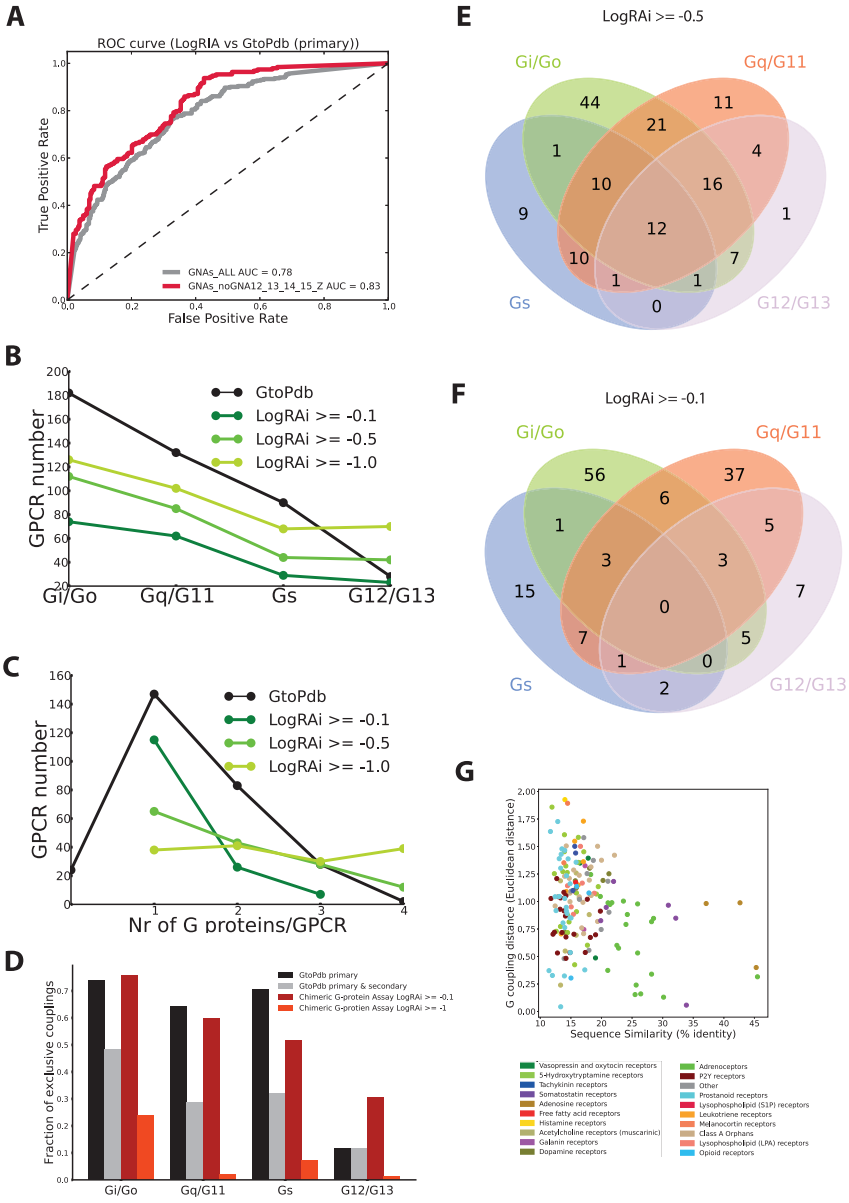

Figure S4. Analysis of the Chimeric G-Protein-Based Assay Dataset and Comparison with GtoPdb, Related to Figures 2 and 3

(A) Roc curve comparing the chimeric G-protein-based TGF-α shedding assay couplings with GtoPdb couplings: roc curves (https://www.scikit-learn.org/) were generated considering only GtoPdb best characterized primary couplings (i.e., reported in at least 3 publications) as binary classifier and TGF-α shedding assay values as scores. Roc curves were calculated either considering coupling values for all the G-proteins in the chimeric G-protein-based TGF-α shedding assay (gray) or by excluding poorly characterized couplings (i.e., GNA12, GNA13, GNA14, GNA15, GNAZ; red curve).

(B) Number of GPCRs coupled to G-proteins of the four families at different LogRAi thresholds in the chimeric G-protein-based TGF-α shedding assay as well as in GtoPdb.

(C) Distribution of the number of reported bindings (of any of the four G-protein families) for each receptor at different LogRAi thresholds in the chimeric G-protein-based TGF-α shedding assay as well as in GtoPdb.

(D-F) Fractions of specific couplings, i.e., receptors binding to members of only one G-protein family, in the chimeric G-protein-based TGF-α shedding assay (dark red and orange bars for LogRAi ≥ -0.1 and -1 couplings) and GtoPdb (black and gray bars for primary only and primary & secondary couplings); Venn diagrams with the numbers of receptors coupled to each G-protein family in the chimeric G-protein-based TGF-α shedding assay at higher LogRAi stringencies ≥ -0.5 (E) and ≥ -0.1 (F).

(G) Comparison of receptor sequence and coupling profile similarities: we calculated receptor pairwise sequence similarity by outputting distance matrices from *ClustalO* (Sievers et al., 2011). We compared receptor pairwise coupling similarity by calculating the distance matrix of coupling profiles (i.e., vectors containing LogRAi values for 11 G proteins) through the *pdist* function from scipy (https://www.scipy.org/).

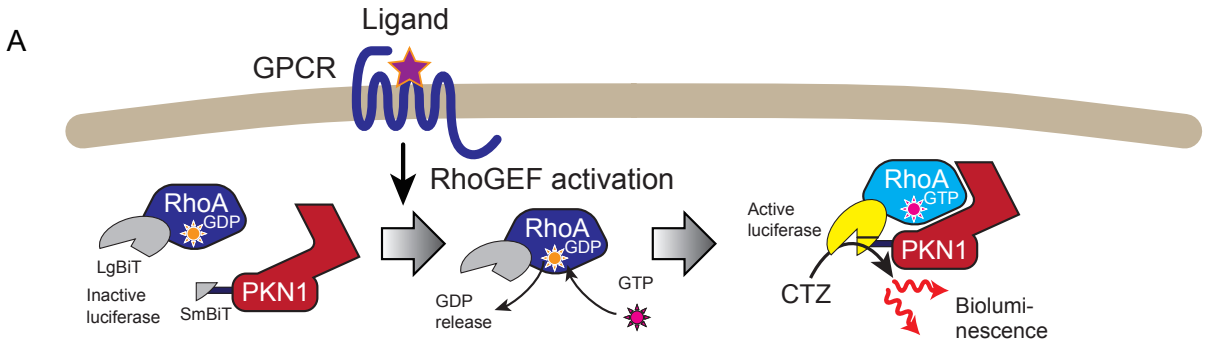

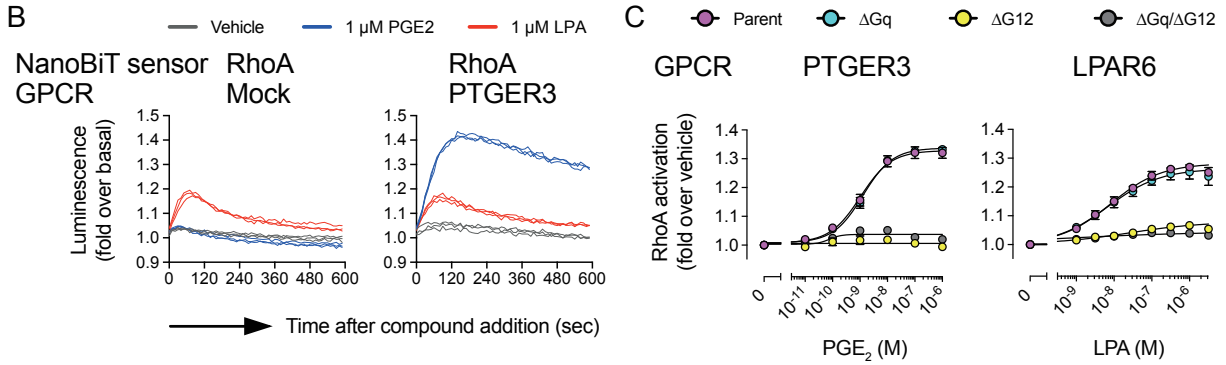

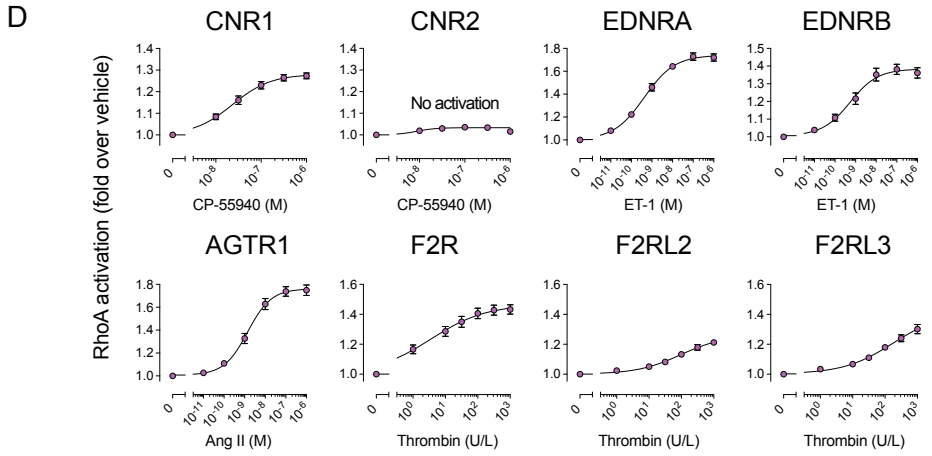

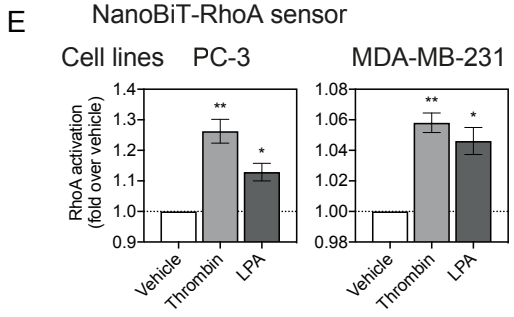

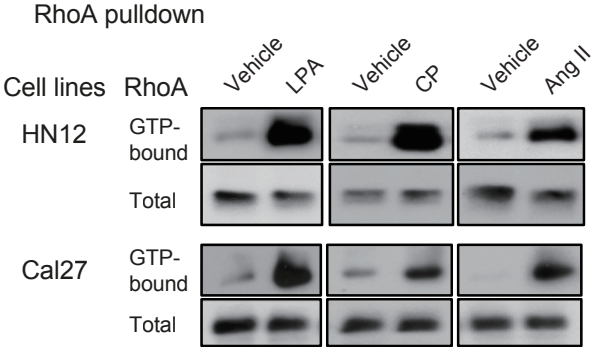

(legend on next page)

Figure S5. Validation of RhoA Activation by the Newly Identified $G_{12/13}$-Coupled GPCRs, Related to Figure 3

(A) Scheme of the NanoBiT-RhoA sensor. The two fragments (LgBiT and SmBiT) of the NanoBiT luciferase are N-terminally fused to RhoA and its effector PKN1, respectively. Upon activation by exchanging GDP to GTP, GTP-bound RhoA interacts with PKN1, thereby increasing luminescent signals being measurable upon loading with CTZ.

(B) Luminescent kinetics of the NanoBiT-RhoA sensor after GPCR ligand stimulation. HEK293 cells expressing the sensor alone (Mock) or with a test GPCR (PTGER3) were stimulated with its ligand (prostaglandin E_2, PGE_2), lysophosphatidic acid (LPA) or vehicle. After ligand addition, a microplate was measured at 10 s interval for 10 min. Each line indicates a luminescent trace of one well, normalized to an initial count, from a representative experiment of at least three independent experiments with similar results. Note that LPA stimulates LPA receptors endogenously expressed in HEK293 cells.

(C) Validation of $G_{12/13}$-mediated signal of the NanoBiT-RhoA sensor. PTGER3 or LPAR6 was expressed with the NanoBiT-RhoA sensor in the parental, ΔG_q, ΔG_{12} and $\Delta G_q/\Delta G_{12}$ HEK293 cells, and ligand-induced luminescent signals were measured. Symbols and error bars represent mean and SEM, respectively, of 4 (PTGER3) and 6 (LPAR6) independent experiments with each performed in duplicate.

(D) NanoBiT-RhoA activation by selected GPCRs. Test GPCRs including the newly identified $G_{12/13}$-coupled GPCRs (Figure 3E) were expressed together with the NanoBiT-RhoA sensor in HEK293 cells and ligand-stimulated luminescent signals were measured. Note that CP-55940-induced RhoA activation occurred in cells expressing CNR1, but not CNR2. Symbols and error bars represent mean and SEM, respectively, of 5-7 independent experiments with each performed in single measurement or duplicate.

(E) NanoBiT-RhoA activation through endogenously expressed GPCRs. PC-3 cells and MDA-MB-231 cells transiently expressing the NanoBiT-RhoA sensor alone were stimulated with vehicle, thrombin (1000 U L^{-1}) or LPA (1 μM), which is a potent inducer of RhoA activation in many cell types. Bars and error bars represent mean and SEM, respectively, of 3 independent experiments with each performed in triplicate. *$p < 0.05$, **$p < 0.01$ as compared with vehicle treatment (one-way ANOVA with Dunnett's post hoc test).

(F) RhoA pulldown assay to detect $G_{12/13}$ activation by endogenously expressed GPCRs. HN12 cells and Cal27 cells were serum-starved and treated with 5 μM LPA, 10 μM CP-55940, 1 μM Ang II or vehicle. Cell lysates were subjected to the pulldown assay using Rhotekin-beads and precipitated GTP-bound RhoA proteins as well as input RhoA proteins (Total) were assessed by immunoblot analysis. Images of immunoblot membranes are representatives of two experiments with similar results.

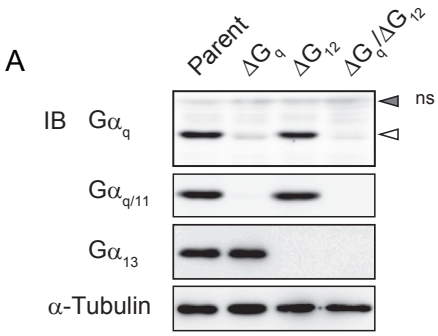

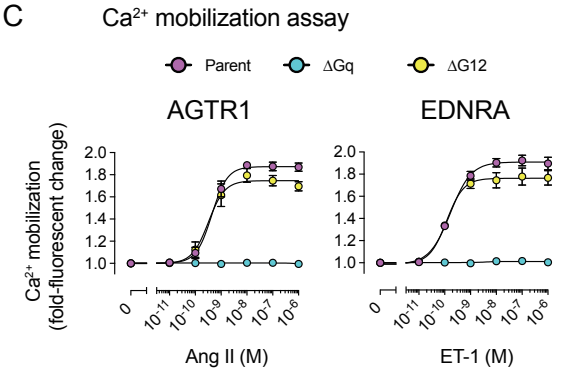

B Chimeric G-protein-based TGFα shedding assay

	AGTR1		EDNRA	
	Parent	ΔG12	Parent	ΔG12
pEC50	9.48 ± 0.06	9.54 ± 0.05t	9.71 ± 0.08	9.56 ± 0.02
E_{max}	57.0 ± 1.6	54.3 ± 2.1	60.9 ± 1.9	58.8 ± 0.8
n =	6	6	4	4

	AGTR1		EDNRA	
	Parent	ΔG12	Parent	ΔG12
pEC50	9.36 ± 0.16	9.44 ± 0.19	9.67 ± 0.06	9.93 ± 0.05
E_{max}	0.87 ± 0.04	0.72 ± 0.04	0.91 ± 0.05	0.77 ± 0.07
n =	4	4	4	4

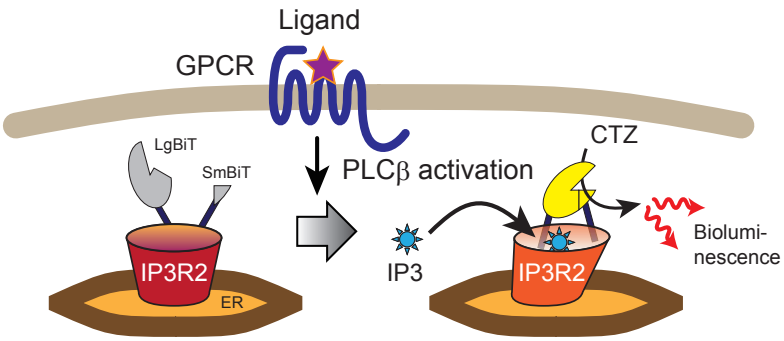

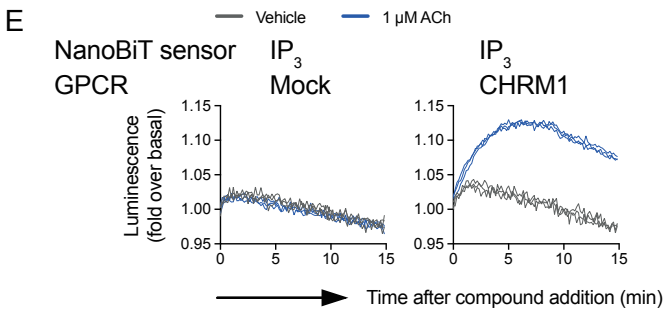

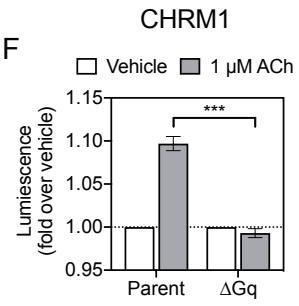

G NanoBiT-IP3 assay

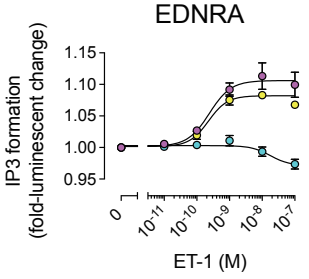

	Parent	ΔG12
pEC50	9.63 ± 0.08	9.68 ± 0.11
E_{max}	0.108 ± 0.019	0.079 ± 0.005
n =	5	5

(legend on next page)

Figure S6. $G_{q/11}$ Signaling in the Absence of $G_{12/13}$ for GPCRs Coupled with $G_{q/11}$ and $G_{12/13}$, Related to Figure 3

(A) Protein expression levels of Gα subunits. Lysates from the parent, ΔG_q, ΔG_{12} and $\Delta G_q/\Delta G_{12}$ cells were subjected to immunoblot analyses using antibodies against $G\alpha_q$ (an open arrowhead), $G\alpha_{q/11}$, $G\alpha_{13}$ or α-tubulin. Note that compensatory upregulation of Gα subunits in ΔG_q cells (for $G\alpha_{13}$) or ΔG_{12} (for $G\alpha_q$ or $G\alpha_{11}$) was not observed. Also, note that owing to a lack of a sensitive, validated antibody against $G\alpha_{12}$, immunoblot for $G\alpha_{12}$ was not assessed. ns, non-specific immunoreactive band (a filled arrowhead).

(B) Parameters obtained from concentration-response curves of the chimeric G-protein-based TGF-α shedding assay (Figure 3E). Parameters are shown as mean ± SEM of the indicated numbers of independent experiments.

(C) Ca^{2+} mobilization assay. The parent, ΔG_q and ΔG_{12} cells transiently expressing AGTR1 or EDNRA were loaded with a Ca^{2+} fluorescent dye and ligand-induced Ca^{2+} mobilization was assessed. Symbols and error bars represent mean and SEM of the indicated numbers of independent experiments with each performed in duplicate. Parameters (mean ± SEM) obtained from the concentration-response curves are shown at the bottom.

(D) Scheme of the NanoBiT-IP_3 sensor. The two fragments (LgBiT and SmBiT) of the NanoBiT luciferase are N-terminally and C-terminally, respectively, fused to inositol-triphosphate (IP_3) receptor IP3R2. Upon activation of phospholipase Cβ and hydrolysis of phosphoinositides, released IP_3 induces conformational change in IP3R2 and increases luciferase activity.

(E) Luminescent kinetics of the NanoBiT-IP_3 sensor after GPCR ligand stimulation. HEK293 cells expressing the sensor alone (Mock) or with a test GPCR (CHRM1) were stimulated with its ligand (acetylcholine, ACh) or vehicle. After ligand addition, a microplate was measured at 10 s interval for 15 min. Each line indicates a luminescent trace of one well, normalized to an initial count, from a representative experiment of at least three independent experiments with similar results.

(F) Validation of $G_{q/11}$-mediated signal of the NanoBiT-IP_3 sensor. The parental or ΔGq cells transiently expressing CHRM1 and the NanoBiT-IP_3 sensor were stimulated with vehicle or ACh, and ACh-induced luminescent signal change was normalized to that of vehicle treatment. Bar and error bars represent mean and SEM, respectively, of 5 (parent) or 4 (ΔG_q) independent experiments with each performed in triplicate. ***$p < 0.001$ (t-test).

(G) Measurement of IP_3 formation in EDNRA. The parent, ΔG_q and ΔG_{12} cells transiently expressing EDNRA and the NanoBiT-IP_3 sensor were stimulated with a titrated ligand and ligand-induced luminescent signal was assessed. Symbols and error bars represent mean and SEM of the indicated numbers of independent experiments with each performed in duplicate. Parameters (mean ± SEM) obtained from the concentration-response curves are shown at the right.

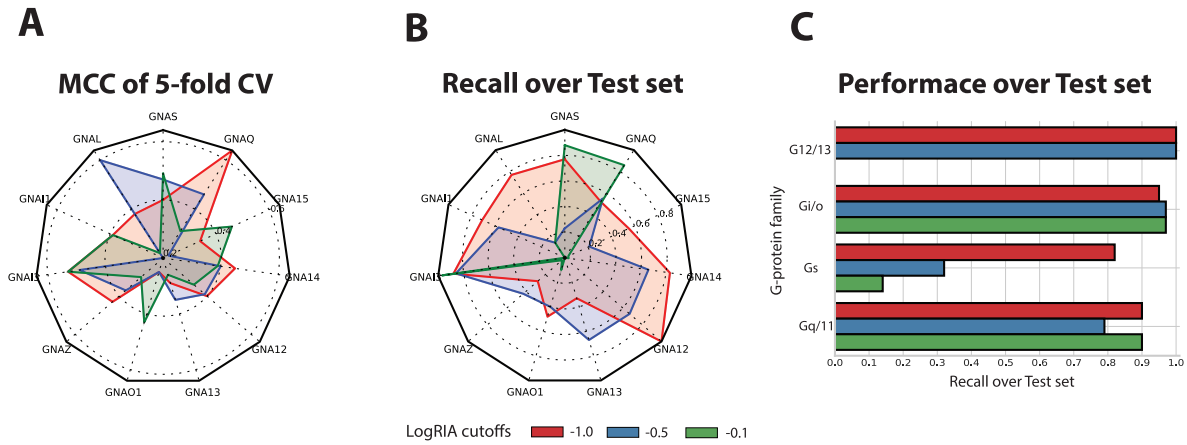

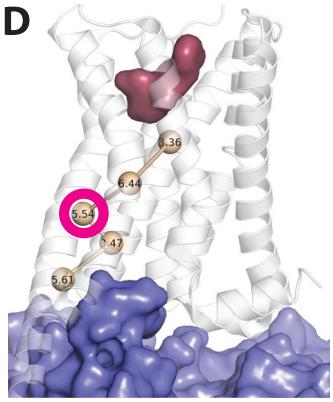

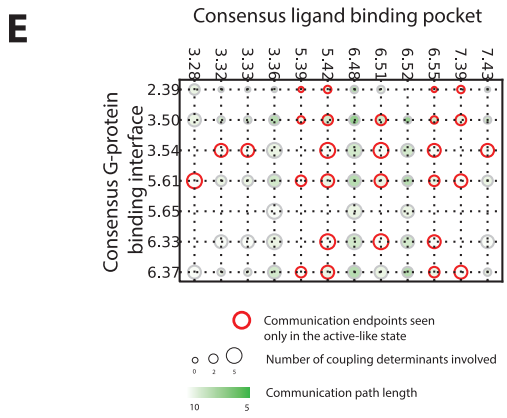

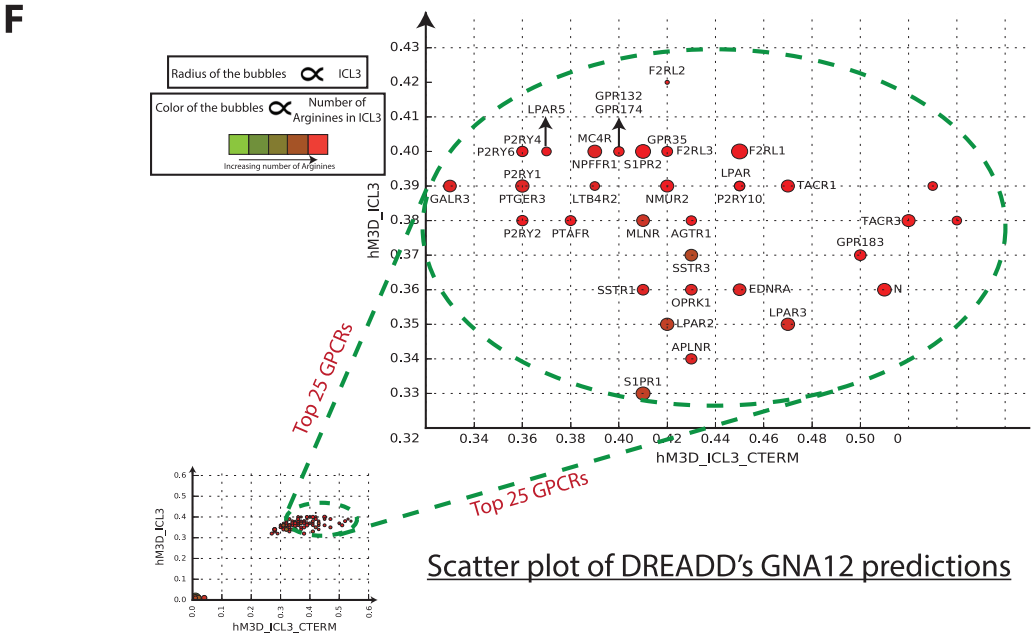

(legend on next page)

Figure S7. Predictor Performances, Shortest Path from Contact Network Analysis, DREADD Predictions Scatterplot, Related to Figures 4, 6, and 7

(A) Radial plot representing Matthew correlation coefficient (MCC) of 5-fold cross validation (averaged over 10 runs).

(B) Radial plot representing Recall (Sensitivity) of the best performing predictors over the Test set.

(C) Bar plot representing the recall (sensitivity) of the best performing predictors, trained at different LogRAi cutoffs, over the test set.

(D) Example of a shortest communication pathway, depicted on 3D cartoons of the *ADRB2-GNAS* complex (PDB: 3SN6), linking the ligand and G-protein consensus binding pocket pockets.

(E) Connectivity matrix displaying shortest paths (as intersecting circles) linking residues forming the ligand and G-protein consensus binding pockets (i.e., shown to form such interfaces in at least 50% of the considered structures). Circle color indicates the path length and the diameter is proportional to the number of significant coupling features found at linking positions. Circle rims are red marked if the path is exclusively found on active-like GPCR structures.

(F) Scatterplot of the relative coupling probabilities of chimeric sequences obtained by swapping on the M3D backbone sequence the sequence stretches corresponding to the ICL3 alone (y axis) or in combination with the C-term (x axis) from the 148 receptors of the chimeric G-protein-based TGF-α shedding assay. The zoomed caption highlights the cluster of chimeric sequences (including GPR183 and GPR132) displaying an increase of coupling probability for GNA12 compared to the reference (i.e., M3D).